SCIENCE CHINA
Technological Sciences

doi: 10.1007/s11431-012-4779-8

Seasonal variations of night mesopause temperature in Beijing observed by SATI4

XIONG JianGang*, WAN WeiXing, NING BaiQi, LIU LiBo, WU BaoYuan, HU LianHuan & XU Tao

Beijing National Observatory of Space Environment, Institute of Geology and Geophysics, Chinese Academy of Sciences, Beijing 100029, China

Received January 26, 2012; accepted February 15, 2012

The data observed by a spectral airglow temperature imager (SATI) at Beijing National Observatory of Space Environment from July 23, 2008 to July 31, 2009 are used to study night mesopause temperature in Beijing. From variations of temperature at 87 and 94 km obtained from OH (6-2) and O_2 (0-1) airglow spectra, temperature at night is shown lowest in the summer and highest in the winter. In summer, average temperature at 87 km is 173.9 K, lower than average temperature 180.1 K at 94 km. But in winter, average temperature at 87 km is 201.2 K, higher than average temperature 194.8 K at 94 km. The altitude of mesopause in Beijing is below 87 km in summer and above 94 km in winter. There are about 120–150 days when the mesopause locates below 87 km, which is in agreement with the results of SABER/TIMED. Variations of temperatures at 87 and 94 km are analyzed by harmonic method. Our results show that amplitudes of annual oscillation of temperature at 87 and 94 km are 17.5 and 7.8 K respectively. Amplitudes of semi-annual oscillation at 87 and 94 km are 1.6 and 5.3 K, which are smaller than those of annual oscillation. Although there are differences among different observations because of different locations and different instruments, our results are in general agreement with observation at similar latitude as Beijing.

mesopause, temperature, airglow, seasonal variations, SATI

Citation: Xiong J G, Wan W X, Ning B Q, et al. Seasonal variations of night mesopause temperature in Beijing observed by SATI4. Sci China Tech Sci, 2012, 55: doi: 10.1007/s11431-012-4779-8

1 Introduction

The mesopause which we take as 80 to 105 km is the layer with minimum temperature in the atmosphere. Since mesosphere is affected by upper and lower atmospheres, variation of mesopause represents partly the variation of atmosphere in the lower and upper regions. Former measurements of temperature in the mesopause showed clear seasonal variation. The temperature in the mesopause reaches its minimum in summer, not the same as that in lower atmosphere, which is related to the meridional circulation driven by the drag of breaking waves propagated from lower atmosphere [1]. The altitude of mesopause over middle and high latitudes can be altered by atmospheric waves [2, 3]. It is important to measure temperature of the mesopause continuously for the study of coupling between lower and upper atmospheres.

Measurements of temperature in the mesopause have long been a challenge. But now some valid instruments can be used to obtain temperatures in the mesopause. Besides direct meteorological rocket observations, including those using falling spheres, the global observation by satellites and ground based observation are two main remote observation methods. Although sounding rocket experiments can get high resolution temperature profiles, the observations

*Corresponding author (email: xjg@mail.iggcas.ac.cn)

are rather sparse. Satellite temperature measurement can provide global profiles but with low resolution of local time [2]. Since high altitude and time resolution temperature profile can be obtained by lidar, narrowband metal lidar became important instrument for the mesopause temperature measurements [4]. Another type of ground based mesopause temperature observation equipment is various airglow spectrometers. Although they can only provide temperatures at several discrete altitudes at night, they have been installed all over the world [5–7], because they can provide good measurement data at low running expense. In China, temperatures measured by lidar and airglow image observed by all-sky imager have been reported [8, 9], but there was no temperature measurement by airglow instrument until 2008.

In 2008, a spatial and spectral imaging Fabry-Perot spectrometer named SATI (Spectral Airglow Temperature Imager) was installed at Beijing Observatory (40.30°N 116.19°E). In this paper, we will report seasonal variation of mesopause temperatures in Beijing based on the observation from July 2008 to July 2009. In the next section, we will introduce briefly the SATI instrument. Seasonal variations of temperature are presented in Section 3. Conclusion is given in Section 4.

2 Instrument and data

Airglow is the very weak emission of light of atoms and molecules. Atoms or molecules are energized by solar UV or X-Ray in the thermosphere, and they emit quanta to be stabilized into lower energy states through quenching or collisions. Although the airglow can be observed globally, it is not noticeable during the daytime since the light of the daytime sky is many orders of magnitude larger. Early SATI instrument (MORTI) can only be used to measure O_2 airglow [10], the new SATI instrument added OH filter to measure the OH (6-2) band airglow [11]. SATI is a sensitive, stable, and convenient sensor of temperature and composition changes in the lower thermosphere/upper mesosphere. The SATI instrument error of temperature measurements is approximately 1.7 K standard deviation [12]. Beijing SATI is one of the newest SATI with different hardware and upgrade software, we also call it SATI4.

The OH (6-2) Meinel band and O_2 (0-1) atmospheric band are chosen for SATI measurements to investigate the MLT region. The OH (6-2) Meinel band of the hydroxyl radical is emitted from layer at about 87 km altitude and the O_2 (0-1) atmospheric band is emitted from layer centered at about 94 km. Both emissions result from the photodissociation of molecular oxygen by solar ultraviolet radiation and the subsequent recombination of the atomic oxygen to molecular form. The three-body process (where M is any third body), $O(^3P)+O(^3P)+M \rightarrow O_2^*+M$ produces an excited state of O_2, denoted O_2^*, and then those excited species exchange energy with O_2, as described by $O_2^* + O_2 \rightarrow O_2(b^1\sum_g^+)+O_2$. The $O_2(b^1\sum_g^+)$ state then radiates in the O_2 atmospheric bands (0-0) and (0-1) by decay to the ground state $O_2(X^3\sum_g^-)$. The (0-0) band emission at 762 nm cannot be observed with ground-based instruments, because it is absorbed by O_2 in the lower atmosphere. On the other hand, the (0-1) band at about 866 nm can be measured from the ground. The O_2(0-1) band has P and R branches, the P branches contain several PP and PQ branches pairs. SATI uses five of them: PP/PQ_5, PP/PQ_7, PP/PQ_9, PP/PQ_{11}, PP/PQ_{13} with wavelength 865.51/ 865.99/866.48/ 866.99/ 867.53 nm to calculate rotational temperature at 94 km. Atomic oxygen is also converted to ozone, leading to the reaction $H+O_3 \rightarrow OH^*+O_2$. The excited OH^* in the upper vibrational levels (such as v'=6, 7, 8, 9) is transferred to lower vibrational levels (such as v''=2), $OH^*(v') \rightarrow OH(v'')$. Meinel bands OH (8-3), OH (7-2), OH (6-2) are frequently used for the mesopause measurement. For SATI the Q branch of the OH (6-2) band is chosen at about 835 nm. SATI uses three main Q branches $Q_1(1)/Q_1(2)/Q_1(3)$ with wavelength 834.46/835.29/836.47 nm to calculate rotational temperature at about 87 km.

The SATI instrument resolves the integrated emission rates of the rotational lines in the above-mentioned Meinel and atmospheric bands. A detailed structure and principle introduction of SATI can be found in ref. [11]. Main parameters of SATI4 are listed in Table 1. The SATI configuration can be divided into three parts: collecting, filtering, and imaging. Two narrow-band interference filters on a filter wheel and a CCD camera are used for the filtering and imaging, respectively. For the light collection, SATI uses a conical mirror and a Fresnel lens. Only light with zenith angle between 26.3° and 33.8° can be reflected off the conical mirror and reaches an interference filter after passing through a Fresnel lens. That means the field of view (FOV) of SATI is an annuluson the sky, the central radius of FOV is 50 km for OH (6-2) airglow at 87 km and 54 km for O_2 (0-1) airglow at 94 km. SATI4 installed in Beijing operates with exposure time 120 s for each measurement, so the time resolution is about 4 min for two airglow layers. A dark current image is taken for every 10 airglow images (five OH and five O_2 airglow images). Figures 1(a) and 1(b) show the typical OH and O_2 images. There are three bright circles in OH image corresponding to three OH (6-2) bands $Q_1(1)/Q_1(2)/Q_1(3)$. Five bright circles in O_2 image correspond to five O_2 (0-1) spectra peaks PP/PQ_5, PP/PQ_7, PP/PQ_9, PP/PQ_{11}, PP/PQ_{13}. After subtracting dark current image and making flat-field correction, we use synthetic spectra or modeled spectra to find the spectrum that best fits the observed spectrum. The synthetic spectra $S_{syn}(\lambda,T)$ are functions of temperature T and wavelength λ [11]. Using $ES_{syn}(\lambda,T)+B$ to fit the observed spectrum $S_{obs}(\lambda)$, temperature at 87 km or 94 km is just the temperature corresponding to the best fit synthetic spectra of OH or O_2. The

Table 1 SATI4 instrument specifications

Parameter	Value
Annular field of view	26.3° to 33.8°
O_2 channel central wavelength	868.00 nm
OH channel central wavelength	836.90 nm
FWHM	0.25 nm
Transmittance at $\theta = 0°$	52.07%
Transmittance at $\theta = 9.8°$	43.35%
CCD type	(E2V CCD57-10)
CCD size	6.66mm×6.66mm
Lens type	Navitar
Lens parameter	17mm F0.95
Typical integration time	120 s
Environment temperature range	10–25°C

emission rate E and background B can also be obtained simultaneously.

In this study, temperatures by the SABER (Sounding of the Atmosphere by Broadband Emission Radiometry) instrument [13] are used to compare the SATI4 temperature. SABER is a 10-channel radiometer, launched on the TIMED (Thermosphere-Ionosphere-Mesosphere Energetics and Dynamics) satellite in December 2001, providing near-global measurements of infrared and near-infrared emissions. The temperatures from 20 km to 120 km can be retrieved from the emissions. The SABER temperatures at 94 and 87km used here are average temperatures in 3 km height centered at 94 and 87 km, respectively.

3 Results and discussion

3.1 Observation

Temperatures mentioned in this study are night temperatures, since SATI can only run at evening time without moonlight. Figure 2 shows temperatures at 87 and 94 km estimated from the OH and O_2 airglow images on October 27, 2008. SABER temperatures are also shown in the figure. All the SABER observations in a range centered at Beijing with radius 5° are chosen to compute average temperature and average time as the temperature and time that SABER flies over Beijing. SABER flies over Beijing two times every day, but we only use the temperatures at night. On October 27, 2008, SABER passed over Beijing at 18:40 UT (02:40 LT, October 28) in the evening. Temperatures obtained from OH and O_2 airglow by SATI4 were almost the same as those by SABER at 18:40 UT. Generally, SABER temperatures are accepted as good measurement for the middle atmosphere with error less than 5 K. That indicates that SATI4 measurements in Beijing are reliable. We will later show difference between SATI and SABER temperatures in a whole year.

Comparing the temperatures at 87 and 94 km, night

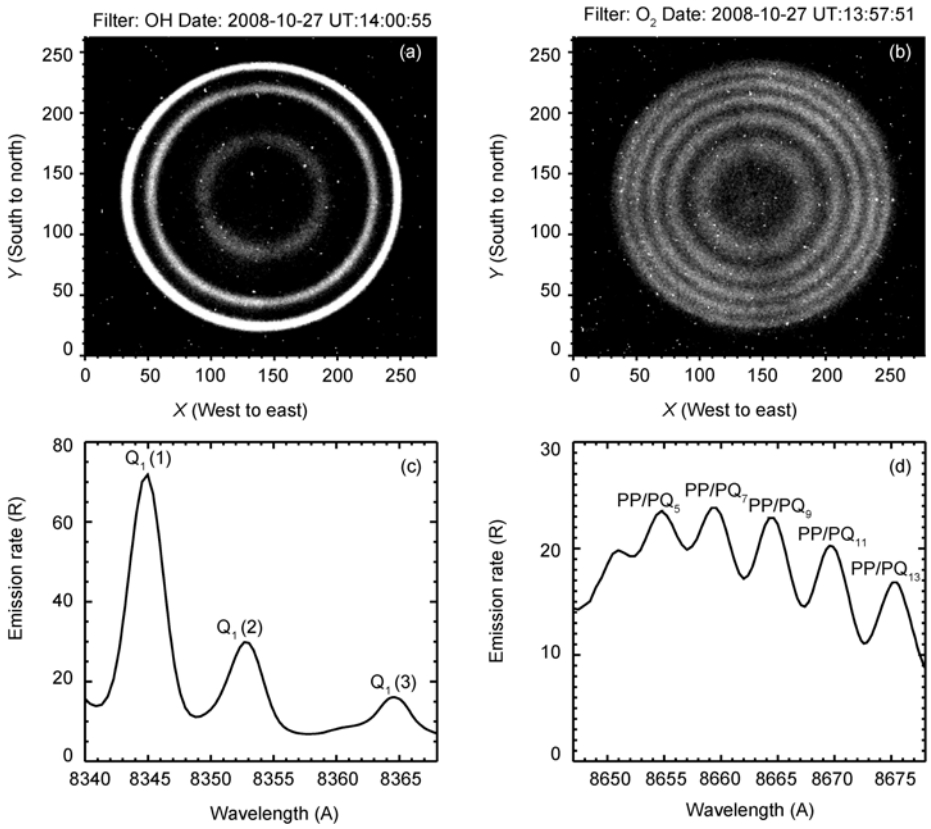

Figure 1 Airglow images and spectra at night on October 27, 2008.

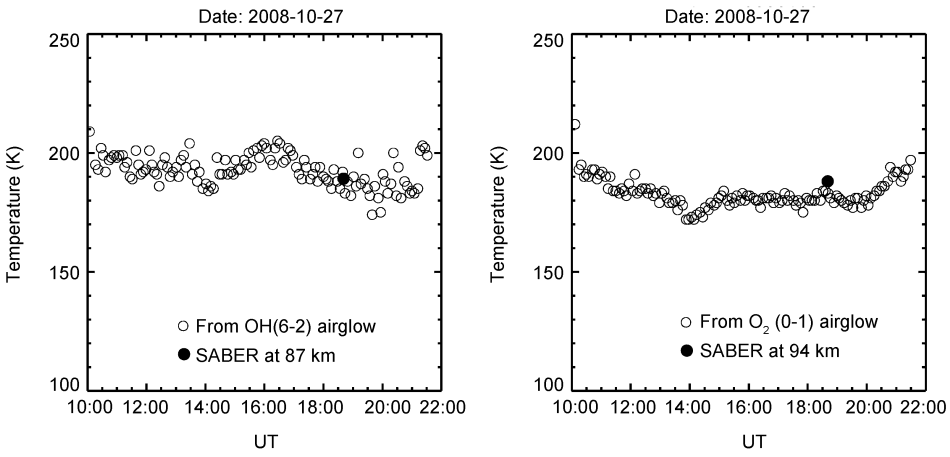

Figure 2 Temperatures at 87 and 94 km in Beijing at night on October 27, 2008.

average temperature at 87 km is higher than that at 94 km. Since temperature increases with altitude below mesopause and decreases with altitude above mesopause, mesopause on October 27, 2008 must be higher than 94 km or quite near 94 km. Some other observations have shown that mesopause in winter was at about 100 km [2, 14]. So the mesopause on October 27 was above 94 km.

We can find temperature disturbances at 87 and 94 km from Figure 2. Those may be the results of tides or/and gravity waves. Temperature from a whole image is average temperature of the annulus as mentioned above. The annulus can also be divided into several sectors. From the image of every sector, temperature and emission rate at every sector can also be deduced using the same method. Generally, we divide the annulus into 12 sectors, then 12 temperatures at different positions in the sky can be obtained. Those positions are on a circle with radius 50 and 54 km at altitudes 87 and 94 km, respectively. Figure 3 shows the temperatures at 12 positions at 87 km from the OH airglow image. Correlated variation in different sectors can be seen from the temperature variation. Parameters such as period, horizontal wavelength and propagation direction can be obtained using suitable methods [15]. The statistic results of the gravity wave parameters will be published elsewhere, and we only use the average temperature in a whole year to study seasonal variation of temperatures in Beijing.

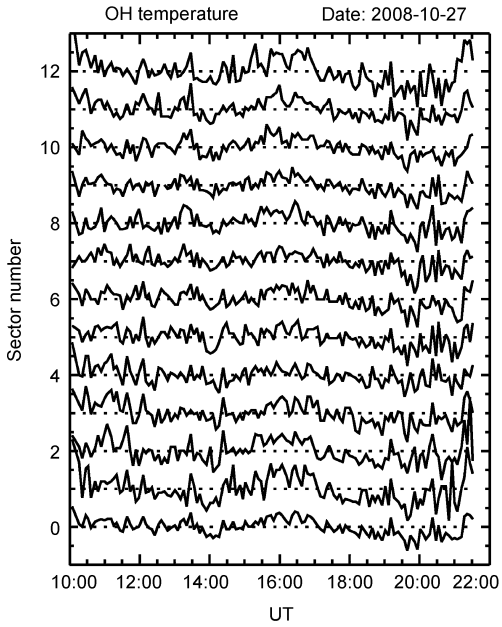

Figure 3 Temperatures at different sectors at 87 km in Beijing.

3.2 Temperature comparison

To compare SATI4 and SABER measurements from July 23, 2008 to July 31, 2009, we first calculated two universal times when SABER traversed over Beijing with ascending and descending orbits, respectively. If there were valid SATI measurements within one hour of any of the above times, we compared the measurements of SATI and SABER. Figure 4 shows the results. Differences between the two measurements are also shown in the figure. It can be seen that for the whole year, SATI4 and SABER temperatures at 87 and 94 km followed a similar variation, i.e., temperatures were low in summer and high in winter. Average differences of the two measurements were 0.53±11.8 K and 0.44±14.8 K at 87 and 94 km, respectively. SATI4 temperatures in winter were a little higher than SABER and those in summer were a little lower than SABER. But average differences were quite small by both instruments. Figure 4 also shows the fit of temperatures by SATI4 and SABER. The fit includes mean, annual and semi-annual variations. The results also show similar variation and small difference by two instruments.

López-González el al. [16] compared temperatures of four years measured by SABER with SATI placed at Sierra Nevada Observatory (37.06°N, 3.38°W) and found that the differences were –6.8±9 K and –2.1±10 K at 87 and 94 km. Comparison of the temperatures measured by SABER and

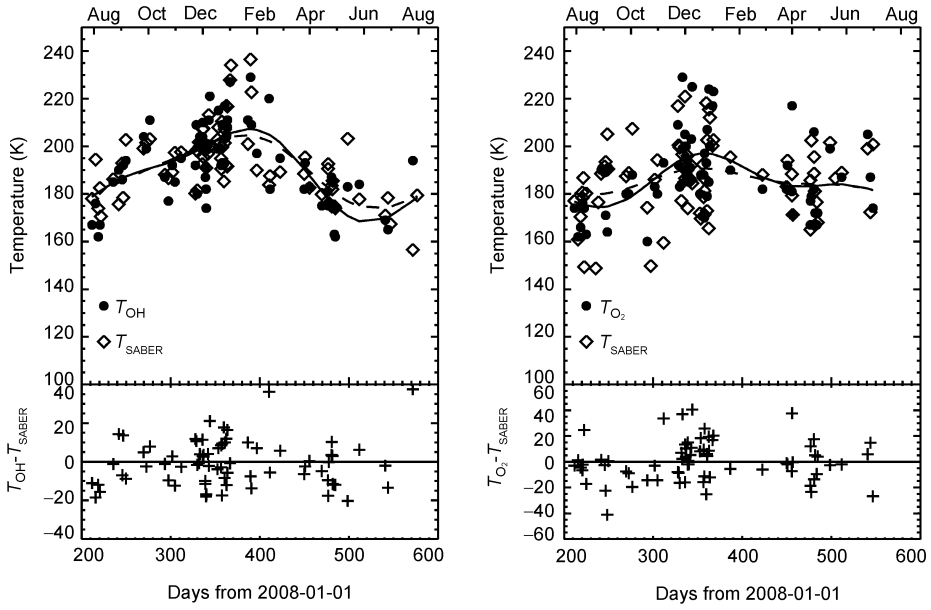

Figure 4 Comparison of temperatures at 87 and 94 km observed by SATI and SABER.

OH (3-1) rotational temperatures at 51.3°N, 7.2°E in Germany showed that the difference was −7.5±7.5 K at 87 km [17]. All of the observations including SATI4 in Beijing showed similar temperature variation with seasons. Rotational temperatures from airglow are average temperature at the emission layers, the contributions from different altitudes are not the same. It is not easy to calculate SABER with the same weight as airglow temperature. The altitude of OH emission layer and bandwidth may have some variations; this is another reason for comparison of differences.

3.3 Seasonal variation

We averaged all temperatures by SATI4 at every month. Then we obtained average temperatures for all months of a year. In fact, average temperatures in January to June and August to December were from a month in 2008 or 2009. But average temperature in July was average temperature in July 2008 and July 2009. The measurement from July 23, 2008 to July 31, 2009 covered a whole year. The results including fitting curve with annual and semi-annual variations are shown in Figure 5. The error bars indicate standard deviation of temperatures from averages. Table 2 shows day numbers at every month, when there were more than 20 valid images at night. There were 125 nights and 120 nights with more than 20 OH and O_2 images in a night. In summer, measurement days were less than in winter. That is the reason for relative large error bar in summer months. Some error bars are so long that temperatures at 87 and 94 km may overlap with each other. In the figure, temperatures at 87 km shift right in time abscissa in order to distinguish the temperatures at different altitudes.

During July 2008 to July 2009, average annual temperature in Beijing at 87 and 94 km was 188±13 K and 185±8 K. Compared with other observations, such as 190 K at 87 km at 42°N [18], 198 K at 87 km at 35°N [19], 202 K at 87 km at 37°N [6], and 190 K at 94 km at 37°N [6], results by SATI4 in Beijing are reasonable.

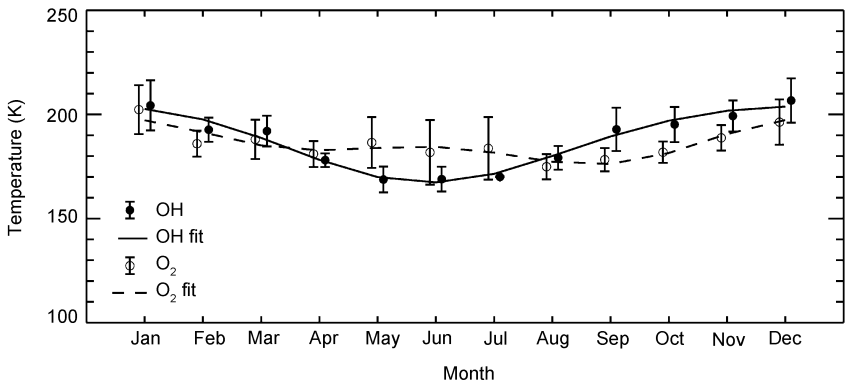

Figure 5 Seasonal variations of temperatures in Beijing, temperatures at 87 km shift right avoiding overlap in the figure.

Table 2 Day numbers with valid images more than 20 in one night

	Jan	Feb	Mar	Apr	May	Jun	Jul	Aug	Sep	Oct	Nov	Dec	Total
OH	13	10	9	10	8	7	2	9	11	11	18	16	125
O_2	6	5	8	6	5	5	2	9	12	11	17	14	100

At 87 km, average temperature was 173.9 K in summer months (June, July and August) and 201.2 K in winter months (December, January and February). At 94 km, average temperature was 180.1 and 194.8 K in summer and winter months. Temperatures in winter at both altitudes were higher than in summer. This seasonal temperature variation is in contrast to the temperature variation in lower atmosphere. Mesopause structure is formed by atmospheric radiation, chemical heating and dissipation, but strong gravity wave activity in summer can change mesopause structure. When strong gravity waves broke above 80 km, large-scale meridional circulation from summer to winter hemisphere was driven. Then the air in the summer atmosphere experienced upward vertical motion accompanied by adiabatic cooling in mesopause. This characteristic is also shown in SABER measurements [2].

In winter, temperature at 87 km was higher than at 94 km, that means mesopause in Beijing is above 94 km. Measurement on October 27, 2008 also showed that (as in Figure 2). But in summer, average temperature at 87 km was lower than at 94 km. That means summer mesopause is below 87 km. Von Zahn et al. [3] first found global two-level structure of mesopause, i.e., mesopause in summer hemisphere at high and middle latitudes was near 86 km, but it was near 100 km in winter hemisphere and in summer hemisphere at lower latitude. The transition latitude was at 24° in summer hemisphere. Xu et al. [2] indicated that two mesopause altitudes were at 95–102 km and 82–85 km, the transition latitude was located between 30–40° in day and 25–30° at night based on SABER observation. Average temperature shown in Figure 5 is night average temperature. SATI4 measurement fits SABER observation very well. Formation of lower mesopause in high and middle summer hemispheres is also related to the strong gravity wave activity in high latitude summer hemisphere, and tidal modulations [2]. In about 120 to 150 days from April to August, temperature at 87 km was lower than at 94 km. That day length is also consistent with SABER observation.

In Figure 5, dash lines represent fitted temperatures as

$$T = T_0 + T_1 \cos\left(\frac{2\pi M}{12} + \phi_1\right) + T_2 \cos\left(\frac{2\pi M}{6} + \phi_2\right),$$

where M is month, T_0, T_1, T_2 represent mean temperature, annual and semi-annual amplitudes, ϕ_1, ϕ_2 represent annual and semi-annual phases. Results are listed in Table 3. Annual variations were greater than semi-annual variations at both altitudes. At 87 km, annual amplitude was 10 times greater than semi-annual amplitude. Temperature at 87 km was obviously minimum in summer and maximum in winter. At 94 km, the difference between annual amplitude (7.8 K) and semi-annual amplitude (5.3 K) was much smaller than that at 87 km. The seasonal variation at 94 km is not so large as that at 87 km. She et al. [14] found that annual variation was minimum near mesopause based on the observations by lidar located at Colorado (41°N, 105°W). They showed that annual variations were 41.8 and 15 K at 87 and 94 km, respectively, both were large compared with SATI4 observations in Beijing. Annual amplitudes at 87 and 94 km at Granada (37.06°N, 3.38°W), Spain, by a SATI were 14 and 9 K. Semi-annual amplitudes were 3 and 4.3 K respectively [6]. Their results were close to observations in Beijing as shown in Table 3. SABER measurement from 2002 to 2006 showed that the annual and semi-annual variation at 40°N at 85 km were 15.8 and 2.35 K [2].

Table 3 Annual and semi-annual amplitudes of temperatures in Beijing

Altitude (km)	Annual amplitude (K)	Semi-annual amplitude (K)
87	17.5	1.6
94	7.8	5.3

Comparing results by airglow instrument and lidar, people have found that temperature variation by airglow instrument is smaller than by lidar at similar latitude position. The reason for this may be that the temperature obtained from airglow is averaged in airglow emission layer. Different locations and different years can affect the comparison. As shown in Table 2, in some months SATI4 operates only short time at night, tides may affect the obtained average temperatures and increase error of average month temperatures. But seasonal variation of most observation is similarand variation amplitudes by SATI are close to those by other aiglow instrument and SABER.

4 Conclusion

In this study we used temperature by SATI4 located in Beijing to analyze seasonal variations of temperatures at 87 and 94 km. Hydroxyl and molecular oxygen airglow rotational temperatures during July 23, 2008 to July 31, 2009 showed that both temperatures at 87 and 94 km reached maximum in winter and minimum in summer. Average temperatures of the whole year were 188±13 K and 185±8 K at 87 and 94 km, respectively. At 87 km, average temperature was 173.9 K in summer and 201.2 K in winter. At 94 km, average temperature was 180.1 K in summer and 194.8 K in winter. Those results are close to other observations such as airglow

instruments and SABER at similar latitude as Beijing.

A clear annual variation was found in temperature variation, together with a semi-annual variation with small magnitude. Annual amplitudes of temperature were 17.5 and 7.8 K at 87 and 94 km. Semi-annual amplitudes were 1.6 and 5.3 K at 87 and 94 km, respectively. The results are in agreement with other measurements at mid latitudes. The differences among different observations could be the result of different locations and different instruments.

In summer, the result that average temperature at 87 km was smaller than at 94 km shows mesopause located below 87 km. This indicates that lower mesopause layer extends from high latitude to Beijing (about 40°N) in summer at night. In winter, mesopause should be higher than 94 km because average temperature at 87 km was smaller than at 94 km. These results are in agreement with the mesopause structure observed by lidar and SABER.

Temperature by SATI4 also shows semidiurnal variations and wave structure in different image sectors, but those waves were not analyzed here. Further study on the temperature tides and gravity waves will help us to better understand mesopause structure and variations.

This work was supported by the National Natural Science Foundation of China (Grant No. 40974086) and the National Important Basic Research Project (Grant No. 2011CB811405). The authors would like to thank the SABER/TIMED team for the excellent temperature data. Many thanks to Dr. ZHAO Fei and CHO YoungMin for their valuable discussions.

1 Walterscheid R L. Gravity wave transports and their effects on the large-scale circulation of the upper mesosphere and lower thermosphere. Adv Space Res, 2001, 27: 1713–1721

2 Xu J Y, Liu H L, Yuan W, et al. Mesopause structure from thermosphere, ionosphere, mesosphere, energetics, and dynamics (TIMED)/ sounding of the atmosphere using broadband emission radiometry (SABER) observations. J Geophys Res, 2007, 112: D09102, doi: 10.1029/2006JD007711

3 Von Zahn U, H ffner J, Eska V, et al. The mesopause altitude: Only two distinctive levels worldwide? GeophysRes Lett, 1996, 23: 3231–3234

4 She C, Yu J, Chen H. Observed thermal structure of a midlatitude mesopause. Geophys Res Lett, 1993, 20: 567–570

5 Buriti R, Takahashi H, Gobbi D, et al. Semiannual oscillation of the mesospheric airglow at 7.4° S during the PSMOS observation period of 1998-2001. J Atmos Solar-Terr Phys, 2004, 66: 567–572

6 López-González M J, Rodrıguez E, Wiens R H, et al. Seasonal variations of O_2 atmospheric and OH(6–2) airglow and temperature at mid-latitudes from SATI observations. Ann Geophys, 2004, 22: 819–828

7 Won Y I. Polar cap observations of mesospheric and lower thermospheric 4-hour waves in temperature. Geophys Res Lett, 2003, 30: 1377, doi:10.1029/2002GL016364

8 Yu C, Yi F. Atmospheric temperature profiling by joint Raman, Rayleigh and Fe Boltzmann lidar measurements. J Atmos Solar-Terr Phys, 2008, 70: 1281–1288

9 Li Q, Xu J, Yue J, et al. Statistical characteristics of gravity wave activities observed by an OH airglow imager at Xinglong, in northern China. Ann Geophys, 2011, 29: 1401–1410

10 Wiens R, Zhang S P, Peterson R, et al. MORTI: A mesopause oxygen rotational temperature imager. Plan Space Sci, 1991, 39: 1363–1375

11 Sargoytchev S I, Brown S, Solheim B H, et al. Spectral airglow temperature imager (SATI): a ground-based instrument for the monitoring of mesosphere temperature. App Opt , 2004, 43: 5712–5721

12 Shepherd M G, Cho Y M, Shepherd G G, et al. Mesospheric temperature and atomic oxygen response during the January 2009 major stratospheric warming. J Geophys Res, 2010, 115: A07318, doi 10.1029/2009JA015172

13 Russell III J M, Mlynczak M G, Gordley L L, et al. Overview of the SABER experiment and preliminary calibration results. Proc SPIE, 1999, 3756: 277–288

14 She C Y, Chen S, Hu Z, et al. Eight-year climatology of nocturnal temperature and sodium density in the mesopause region (80 to 105 km) over Fort Collins, CO (41°N, 105°W). Geophys Res Lett, 2000, 27: 3289–3292

15 Wiens R H, Wang D Y, Peterson R N, et al. Statistics of gravity waves seen in O_2 nightglow over Bear Lake Observatory. J Geophys Res, 1997, 102: 7319–7329

16 López-González M J, Garciacomas M, Rodriguez E, et al. Ground-based mesospheric temperatures at mid-latitude derived from O_2 and OH airglow SATI data: Comparison with SABER measurements. J Atmos Solar-Terr Phys, 2007, 69: 2379–2390

17 Oberheide J, Offermann D, Russell J M, et al. Intercomparison of kinetic temperature from 15 μm CO_2 limb emissions and OH*(3, 1) rotational temperature in nearly coincident air masses: SABER, GRIPS. Geophys Res Lett, 2006, 33, doi: 10.1029/2006GL026439

18 Choi G, Monson I, Wickwar V, et al. Seasonal variations of temperature near the mesopause from Fabry-Perot interferometer observations of OH Meinel emissions. Adv Space Res, 1998, 21: 843–846

19 Shepherd M. Longitudinal variability of mesospheric temperatures during equinox at middle and high latitudes. J Atmos Solar-Terr Phys, 2004, 66: 463–479